The Anatomy of Alignment: Decomposing Preference Optimization by Steering Sparse Features

Jeremias Ferrao[*]
University of Groningen

Matthijs van der Lende
University of Groningen

Ilija Lichkovski
AI Safety Initiative Groningen

Clement Neo
Apart Research

Abstract

Aligning large language models is critical for their usability and safety. However, the prevailing approach of Reinforcement Learning from Human Feedback (RLHF) induces diffuse, opaque parameter changes, making it difficult to discern what the model has internalized. Hence, we introduce Feature Steering with Reinforcement Learning (FSRL), a transparent alignment framework that trains a lightweight adapter to steer behavior by modulating interpretable features from a Sparse Autoencoder (SAE). First, we demonstrate that FSRL is an effective method for preference optimization and is comparable with current RLHF methods. We then perform mechanistic analysis on the trained adapter, and find that its policy systematically promotes style features over explicit alignment concepts, suggesting that the preference optimization process rewards stylistic presentation as a proxy for quality. Ultimately, we hope that FSRL provides a tool for both interpretable model control and diagnosing the internal mechanisms of alignment.

1 Introduction

Large Language Models (LLMs) are increasingly aligned with human preferences using techniques like Reinforcement Learning from Human Feedback (RLHF) (1). While effective, this process modifies a model's underlying weights, inducing diffuse changes across its vast parameter space. This creates an opaque alignment mechanism that is entangled with the model's core capabilities. When this process yields undesirable behaviors like sycophancy or reward hacking (2; 3), diagnosing the root cause is difficult, hindering our ability to build robust and trustworthy systems. This opacity motivates a clear need for alignment methods that are not only effective but also transparent and auditable.

To address this challenge of opacity, we turn to the field of mechanistic interpretability, which seeks to reverse-engineer the internal computations of neural networks. A central tenet is the *Linear Representation Hypothesis*, which posits that high-level concepts are represented as linear directions in a model's activation space (4). Sparse Autoencoders (SAEs) provide a powerful method for discovering these conceptual directions, decomposing a model's dense activation vectors into a sparse basis of largely monosemantic features (5; 6). These features, representing concepts from "code syntax" to "flattery," can be assigned meaningful explanations through automated techniques (5; 7; 8). The existence of such a feature vocabulary suggests a path beyond passive observation toward active, interpretable model control: if we can reliably identify a model's internal concepts, we can then attempt to manipulate them to control its behavior.

[*]Email for Correspondence: j.lino.ferrao@gmail.com

Preprint.

To this end, we introduce **Feature Steering with Reinforcement Learning (FSRL)**. Our framework is designed to leverage this conceptual vocabulary for control by operating on a frozen base LLM and its corresponding SAE. Freezing these components preserves the semantic integrity of the feature basis, ensuring it remains a stable and interpretable interface for intervention. Upon this foundation, a lightweight adapter network is trained via RL to learn an explicit policy for modulating the fixed SAE features, as illustrated in Figure 1.

In this work, we demonstrate that FSRL is an effective alignment method that successfully optimizes an RLHF preference objective. Our primary contribution is the mechanistic transparency this approach provides. By analyzing the learned policy, we find that the pressures of preference optimization on the UltraFeedback dataset translate into a concrete strategy at the feature level: the policy systematically increases the proportional activation of features related to style and formatting, while decreasing that of features explicitly tied to alignment concepts. This insight reveals how preference optimization can learn to reward stylistic presentation as a proxy for quality. These results establish FSRL as a tool for both lightweight model control and for diagnosing the internal mechanisms of alignment. [2]

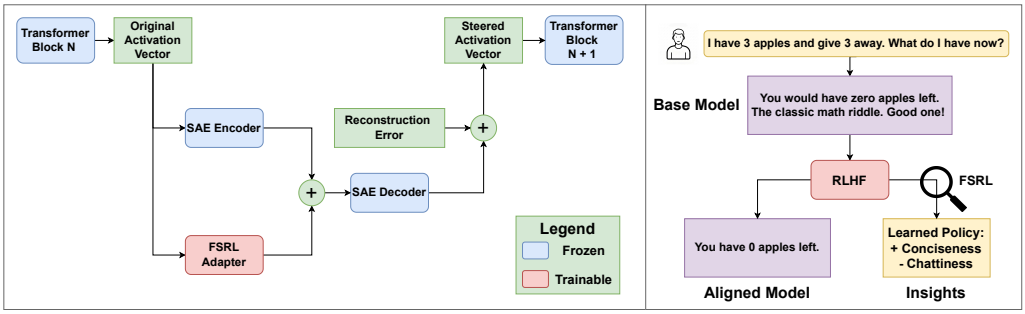

Figure 1: **The FSRL Framework for Interpretable Alignment. (a) FSRL Architecture:** At a given layer, an activation vector is processed by a frozen SAE and a trainable FSRL adapter. The adapter's steering vector is added to the SAE's features, and the resulting activation is reconstructed with the original error term preserved. **(b) Application for Mechanistic Insight:** FSRL replaces opaque alignment processes with a transparent one by learning a policy over a basis of interpretable, monosemantic SAE features. This allows the learned alignment pressures to be decomposed into concrete actions on meaningful concepts.

2 Related Work

Inference-time interventions: Inference-time strategies to modulate model behavior have proven to be a promising alternative to full fine-tuning, which presents a computational burden and introduces complexities like catastrophic forgetting. Techniques such as (contrastive) activation addition (9; 10) inject an activation vector corresponding to certain behaviors or concepts into the residual stream, thereby modifying the model's generation in the desired direction. This technique is statically dependent on the specified behavioral vector; in contrast, it is possible to instead apply a dynamic, context-sensitive intervention by training a controller network to selectively apply a "refusal" vector at inference time (11), and by cross-utilization of steering vectors from a previously aligned model to steer a target model (12). Notably, recent work has introduced an automated steering method whereby internal representations with a high likelihood of yielding unsafe outputs are selectively intervened upon by a refusal head (13). A key innovation in model interventions are Sparse Autoencoders (SAEs), which decompose a model's activations into a sparse basis of monosemantic features (5). Although recent work has questioned the usefulness of SAEs for interpretability (14), the ability of SAE features to causally affect outputs (15) highlights their usefulness as steering targets.

[2]To ensure reproducibility, we provide our code and the evaluated FSRL adapter anonymously. The source code is available at `https://anonymous.4open.science/r/FSRL-MechInterp/README.md`, and the trained adapter with feature classifications can be downloaded from `https://pixeldrain.com/u/bgtHFKDf`.

The goal with FSRL is to combine the strengths of SAEs for interpretability with the promise of learned steering vectors for behavior modification. FSRL's novelty lies within 1) a context-aware application of steering interventions as opposed to static steering vectors, and 2) doing so onto interpretable targets, rather than opaque behavioral targets. By training a network that maps activations to context-specific steering vectors acting on SAE features, we can observe how the pressures of a broad alignment objective decompose into concrete feature-level interventions.

Preference optimization: The challenge of ensuring the outputs of language models adhere to human preferences is foundational to both utility and safety. The standard paradigm for aligning large language models with human values is RLHF. Unlike supervised fine-tuning (SFT), which constrains a model to imitate a static dataset, RLHF involves optimizing a policy (16) against a learned reward signal (1). This optimization process, while powerful, is also a source of vulnerability. Since the reward model is an imperfect proxy for human intent, models can develop undesirable and potentially harmful behaviors (2; 3). A notable modification to the RLHF algorithm was introduced with Direct Preference Optimization (17), which simplifies RLHF by directly optimizing against a classification loss, yielding an efficiency improvement over PPO (16).

Policy optimization algorithms can also intervene on the model at inference-time. Successive Policy Iterations (SPI) applies policy optimization at inference time by searching over value functions to guide the model (18). Along similar lines, Bi-directional Preference Optimization tackles steering as a reinforcement learning task and finds the optimal hyperparameters for contrastive steering by maximizing the likelihood of outputting the target behavior while minimizing the likelihood of the opposite. Our method aligns with SPI and BiPO in its utilization of policy optimization techniques to learn optimal inference-time interventions, but crucially, differs by operating on features extracted by an SAE. This introduces interpretability benefits unavailable with other RLHF methods.

3 Background

Our work combines three key techniques: SAEs for creating an interpretable interface, Simple Preference Optimization (SimPO) for alignment, and a specific preference dataset to train our system.

3.1 Sparse Autoencoders

Sparse Autoencoders (SAEs) are an unsupervised method used to decompose a model's high-dimensional internal activations into a sparse, overcomplete basis of features (5; 19). An SAE consists of an encoder and a decoder. The encoder maps the input activation $\mathbf{x}$ to a sparse feature activation vector $\mathbf{f} \in \mathbb{R}^{d_{\text{sae}}}$, where the feature dimensionality d_{sae} is larger than the model's hidden dimension d. The decoder then reconstructs the original activation, $\hat{\mathbf{x}}$, from $\mathbf{f}$. This process can be described as:

$$\mathbf{f} = \text{ReLU}(W_{\text{enc}}\mathbf{x} + \mathbf{b}_{\text{enc}}) = \text{Encoder}(\mathbf{x}), \tag{1}$$

$$\hat{\mathbf{x}} = W_{\text{dec}}\mathbf{f} + \mathbf{b}_{\text{dec}} = \text{Decoder}(\mathbf{f}), \tag{2}$$

where $W_{\text{enc}} \in \mathbb{R}^{d_{\text{sae}} \times d}$ and $W_{\text{dec}} \in \mathbb{R}^{d \times d_{\text{sae}}}$ are the weight matrices, and $\mathbf{b}_{\text{enc}}$ and $\mathbf{b}_{\text{dec}}$ are bias vectors. The columns of the decoder matrix, W_{dec}, form the dictionary of learned feature vectors.

Sparsity in the feature activations $\mathbf{f}$ is induced by adding an ℓ_1 penalty to the reconstruction loss. The total loss function is therefore:

$$\mathcal{L}(\mathbf{x}) = \|\mathbf{x} - \hat{\mathbf{x}}\|_2^2 + \alpha\|\mathbf{f}\|_1, \tag{3}$$

where α is a hyperparameter that controls the trade-off between reconstruction fidelity and sparsity. While this formulation is common, other SAE variants achieve sparsity through different mechanisms, such as the discontinuous JumpReLU activation function (6) or the Top-K operator (20).

3.2 Simple Preference Optimization (SimPO):

SimPO is an efficient algorithm for aligning language models with human preferences (21). It operates on a dataset $\mathcal{D}$ of preference triplets (x, y_w, y_l), where x is a prompt, y_w is the preferred (winning) response, and y_l is the less preferred (losing response). Unlike the traditionally used Direct

Preference Optimization (22), SimPO does not require a separate reference model, reducing the computational resources required to train a model.

The objective is a modified Bradley-Terry loss with a target reward margin γ, which encourages the model to confidently separate y_w and y_l:

$$\mathcal{L}_{\text{SimPO}}(\pi_\theta) = -\mathbb{E}_{(x,y_w,y_l)\sim\mathcal{D}}\left[\log\sigma\left(\frac{\beta}{|y_w|}\log\pi_\theta(y_w|x) - \frac{\beta}{|y_l|}\log\pi_\theta(y_l|x) - \gamma\right)\right], \quad (4)$$

where β is the temperature/scaling parameter, $|y|$ the sequence length and $\sigma(\cdot)$ the sigmoid function.

3.3 Preference Datasets and Reward Modeling

The classic RLHF pipeline involves a two-stage process: first, a reward model (RM) is trained on human preference data to predict a reward for a response. Second, this RM is used to fine-tune the LLM policy with an online RL algorithm. This process is computationally intensive and prone to reward hacking, where the policy exploits inaccuracies in the proxy reward model.

In contrast, offline preference algorithms like SimPO operate directly on preference datasets. In this work, we use the UltraFeedback dataset (23). Specifically, we utilize the version of this dataset annotated with the Absolute-Rating Multi-Objective Reward Model framework (24). Our choice of this dataset is motivated by its use in the SimPO paper, which allows for a direct comparison, isolating the impact of our proposed FSRL framework rather than confounding it with dataset variations.

4 FSRL Framework

Our methodology centers on FSRL, a framework designed for transparently aligning an LLM by directly manipulating its learned conceptual representations. This section details the system's architecture, the training procedure, and the experimental configuration used to validate our approach.

4.1 FSRL System Architecture

The FSRL system intervenes at a single layer of a frozen base LLM, replacing an activation vector from the residual stream with a steered counterpart. As illustrated in Figure 1, a given activation vector $\mathbf{x} \in \mathbb{R}^d$ from Transformer Block N is processed along two parallel paths.

SAE Path (Frozen) A pre-trained SAE decomposes the input activation $\mathbf{x}$ into a sparse vector of feature activations $\mathbf{f} \in \mathbb{R}^{d_{\text{sae}}}$.

Adapter Path (Trainable) Concurrently, the same activation $\mathbf{x} \in \mathbb{R}^d$ is passed to a trainable adapter π_ϕ, which outputs a steering vector $\mathbf{v} \in \mathbb{R}^{d_{\text{sae}}}$. The adapter is a single feedforward layer with parameters $\phi = (W_a, \mathbf{b}_a)$, where $W_a \in \mathbb{R}^{d_{\text{sae}}\times d}$, $\mathbf{b}_a \in \mathbb{R}^{d_{\text{sae}}}$:

$$\mathbf{v} = \pi_\phi(\mathbf{x}) = \text{ReLU}(W_a\mathbf{x} + \mathbf{b}_a). \quad (5)$$

Feature Fusion and Reconstruction The original feature activations and the learned steering vector are combined via element-wise addition ($\mathbf{f}' = \mathbf{f} + \mathbf{v}$). To avoid degrading the model's capabilities by discarding information not captured by the SAE's sparse basis, we add the SAE's original reconstruction error back to the output. The final activation $\mathbf{x}_{\text{steered}}$ that replaces $\mathbf{x}$ is therefore:

$$\mathbf{x}_{\text{steered}} = \text{Decoder}(\mathbf{f}') + (\mathbf{x} - \text{Decoder}(\mathbf{f})). \quad (6)$$

4.2 Adapter Training and Experimental Configuration

The adapter's parameters are optimized using the SimPO algorithm (21). To encourage a sparse and interpretable policy, we augment the training objective with an ℓ_1 penalty on the steering vector, controlled by a coefficient α. In addition to this proxy-based sparsity, we also investigated a more direct method using a JumpReLU activation (6) in the adapter to directly optimize the ℓ_0 norm. However, this proved to be difficult to tune within our framework.

We evaluate our approach on the Gemma-2-2B-it model (25) using pre-trained SAEs from GemmaScope (26). For training, we use the UltraFeedback dataset (23) as described in Section 3.3. Our

primary experimental decisions involved selecting the intervention layer and the sparsity coefficient. We first performed a sweep across the transformer's quartiles (layers 6, 12, 18, and 24), hypothesizing that mid-model layers would contain the most relevant abstract concepts for alignment. This sweep confirmed layer 12 as optimal. Subsequently, we swept through a range of α values on layer 12 to identify an elbow point that balanced steering vector sparsity with performance on the SimPO validation loss. This led us to select $\alpha = 2 \times 10^{-2}$. The detailed methodology and results of these sweeps are presented in Appendix A, with our investigation into the JumpReLU adapter detailed in Appendix C. The final training configuration and environment details are provided in Appendix B.

4.3 Comparative Evaluation

To contextualize the performance of our FSRL-steered model, we establish a baseline for comparison. The original SimPO paper reports results on a Gemma-9B model; a direct comparison would be inappropriate due to the difference in model scale. Therefore, to ensure a controlled comparison, we trained our own baseline. This baseline consists of the same instruction-tuned model, but is fully fine-tuned using the standard SimPO algorithm rather than our lightweight adapter. The training configuration for this baseline mirrors that of our FSRL adapter, where applicable, with a decrement in the learning rate to ensure stable convergence during full-model training (see Appendix B).

5 Characterizing the Learned Steering Policy

Before analyzing the conceptual biases of the learned policy, we first characterize its behavior to justify our use of a dynamic adapter. We investigate two key questions: first, is the learned policy complex enough that it cannot be replicated by a simple, static heuristic? Second, does the FSRL adapter learn a policy distinct from the SAE's reconstruction objective?

To investigate whether a simpler heuristic could replicate the adapter's performance, we conducted a controlled ablation study. For each input in the validation set, we computed the full steering vector and created a modified vector by retaining only the top-k% of its components with the largest absolute values. Crucially, this percentage is calculated relative to the total number of features in the SAE dictionary (d_{sae}), not just the non-zero components of the steering vector. All other components were set to zero. We then measured the SimPO validation loss for various values of k. The results are shown in Figure 2.

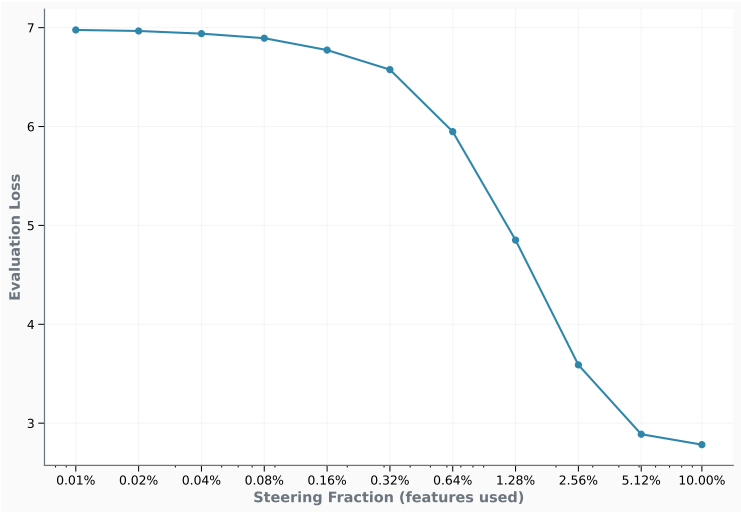

Figure 2: SimPO validation loss as a function of the steering fraction. The fraction (x-axis) is a percentage of the total number of features in the SAE dictionary. For each data point, only the top-k% of steering components by absolute value are retained. This fraction starts at 0.01% and is incremented by factors of two. Performance degrades significantly without a sufficient number of active features.

The results reveal a clear dependence on the number of steered features. Performance is poor with a small steering fraction, and the validation loss only begins to approach its minimum, plateauing after approximately 5% of the total SAE features are retained. This contrasts with our trained FSRL adapter, which achieves its best performance with an average ℓ_0 norm of 930 on the evaluation set, corresponding to activating $\approx$1.42% of the total SAE features per forward pass. The discrepancy suggests that a static, uniform sparsity budget is suboptimal for effective alignment. The adapter, regularized by the ℓ_1 penalty, learns a flexible, input-dependent policy that can apply a highly sparse vector for most inputs but activate a larger set for more complex examples. This finding is further supported by analysis in Appendix D, which shows the adapter's feature usage follows a long-tail distribution.

Next, to determine if the adapter actively modifies the SAE's representations, we analyze the mean difference between the original SAE feature activations ($\mathbf{f}$) and the adapter's steering vector ($\mathbf{v}$) on the UltraFeedback evaluation set (Figure 3). A mean difference near zero would suggest the adapter acts as an identity mapping on average.

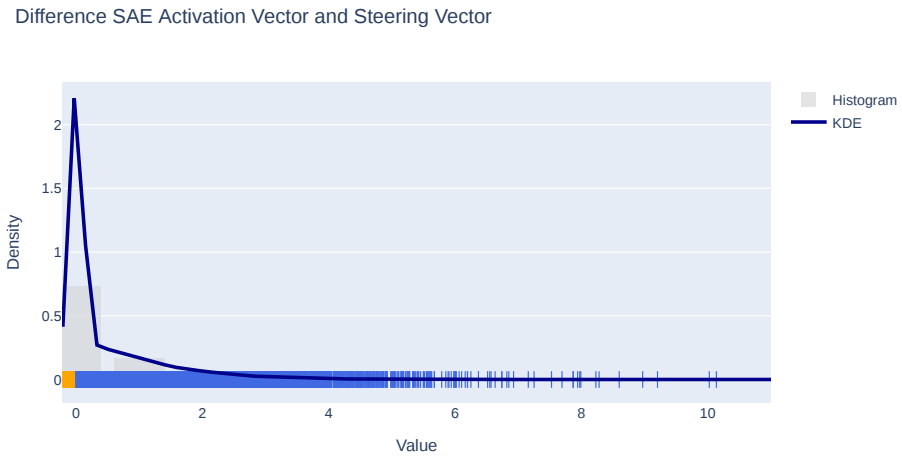

Figure 3: Mean difference between the FSRL steering vector and SAE feature activations, averaged over the UltraFeedback evaluation split. The non-zero mean indicates the adapter learns a policy distinct from the SAE's objective. For readability, 5 features with values > 10 are not shown.

The observed non-zero mean demonstrates that the adapter systematically counteracts or amplifies specific SAE activations. While the magnitudes of these differences are small, this is an expected consequence of the ℓ_1 penalty used for optimization, which encourages many small adjustments rather than a few large ones. This confirms that the adapter learns a distinct policy tailored to minimizing the SimPO loss, rather than simply reproducing the SAE's output.

Together, these results establish that FSRL learns a non-trivial, context-dependent policy that actively reshapes the model's internal representations in a manner that cannot be replicated by simple, static interventions. This justifies the use of a learned adapter for achieving broad alignment objectives.

6 Evaluating Alignment Efficacy

To evaluate FSRL, we compare its performance on standard benchmarks against two models: the base Gemma-2-2B-it model and the same model fully fine-tuned with the SimPO algorithm. The fully fine-tuned model represents the standard, non-interpretable approach to alignment. The goal of this evaluation is not to demonstrate that FSRL can match the performance of full fine-tuning, but to show that it is an effective method for improving preference scores despite operating through a constrained, interpretable interface.

We assess performance on MMLU (27) for general knowledge, TruthfulQA (28) for truthfulness, and GSM8K (29) for mathematical reasoning. Evaluations were performed using the Language Model

Evaluation Harness (30). The results, including the final SimPO loss on the UltraFeedback evaluation set (2.19 for the fine-tuned baseline and 2.73 for our adapter), are presented in Table 1.

Table 1: Benchmark performance. The final SimPO evaluation loss for the fully fine-tuned model and the FSRL-steered model was 2.19 and 2.73, respectively. FSRL improves preference-aligned capabilities while better preserving reasoning compared to full fine-tuning.

Model	MMLU ↑	TruthfulQA (MC2) ↑	GSM8K ↑
Gemma-2-2B-it (Base)	30.14 ± 0.38	55.75 ± 1.58	$\mathbf{53.15 \pm 1.37}$
Gemma-2-2B-it (SimPO Full)	$\mathbf{50.28 \pm 0.40}$	$\mathbf{61.35 \pm 1.63}$	4.40 ± 0.56
Gemma-2-2B-it (FSRL)	38.12 ± 0.40	58.50 ± 1.62	30.40 ± 1.27

As shown in the table, both alignment methods successfully reduce the SimPO loss, confirming they optimize the preference objective. The performance changes align with the patterns documented by Meng et al. (21), where SimPO tuning is expected to improve scores on benchmarks like TruthfulQA while degrading mathematical reasoning on GSM8K. Our FSRL-steered model follows these trends, validating its efficacy as an alignment method.

The comparison between FSRL and full fine-tuning illustrates a trade-off inherent to the optimization process. The fully fine-tuned model achieves a lower preference loss, which corresponds to larger gains on MMLU and TruthfulQA, but also a more severe degradation of reasoning capability. FSRL also improves alignment, resulting in a different point on this trade-off spectrum, with more moderate gains on some benchmarks and less capability degradation on others. The key result is that FSRL is an effective alignment method that provides mechanistic transparency, a primary goal of this work.

7 Mechanistic Insights into the Alignment Process

Having established that FSRL is an effective and dynamic alignment method, we now leverage its primary advantage: interpretability. To analyze the policy at a conceptual level, we developed an automated pipeline to classify SAE features based on their text-based explanations. We focus on two primary categories: 'alignment' features, which encompass concepts such as ethics, safety, and honesty, and 'style' features, which relate to text structure, punctuation, and formatting. This automated process was validated against manual annotations on a random sample of features, achieving a Matthews Correlation Coefficient of 0.448 for alignment features and 0.764 for style features. This indicates a reliable agreement with human judgment (details in Appendix E).

A key consideration for our analysis is that the FSRL adapter and the base SAE operate at different average sparsity levels; the adapter activates a larger set of features on average than the SAE does for reconstruction. Therefore, a direct comparison of feature activation counts would be misleading. To account for this, our analysis focuses on the composition of the active feature set. For any given input, we measure the proportional representation of each category within the set of currently active features. This relative measure allows for a fair comparison of the policy's biases, independent of the overall ℓ_0 norm.

Our primary analysis, summarized in Table 2, was conducted across all token positions of the UltraFeedback evaluation set to ensure the findings are generalizable and not an artifact of the training distribution. The results reveal a clear pattern in the adapter's learned biases: it steers style and formatting features 2–4% more frequently than their baseline proportion in the SAE, while steering alignment-related features 5–11% less frequently. This suggests that the SimPO objective, as defined by the preference data, is achieved more by modulating stylistic presentation than by directly promoting high-level alignment concepts. The reduction in the relative activation rate of alignment features does not imply their suppression; rather, it indicates these features were less instrumental for satisfying the optimization goal compared to features controlling style. The policy learns that enhancing formatting is a more direct path to reward on this dataset.

Our finding that the alignment policy actively promotes style and formatting features provides a direct mechanistic explanation for recent observations in large-scale human preference evaluations. Chiang et al. (31) demonstrated that model rankings on the popular Chatbot Arena benchmark shift significantly when stylistic factors, such as response length and markdown usage, are controlled for in the evaluation. This observation is particularly salient as a model trained by Meng et al. (21) with

Table 2: Aggregate steering effect on the composition of active features. 'SAE Baseline' is the average proportion of active features belonging to a category for the unmodified model. 'Relative Change' is the percent change in this proportion caused by the FSRL adapter. The final column indicates the direction of this change. For context, Alignment and Style features constitute 17.05% and 23.55% of the total classified features, respectively, providing a simple proportional baseline.

Feature Type	Data	SAE Baseline (%)	Relative Change (%)	Improvement
Alignment	Prompt + Chosen	17.59 ± 0.03	-9.42 ± 0.25	$\times$
	Prompt Only	17.10 ± 0.06	-5.47 ± 0.45	$\times$
	Prompt + Rejected	17.53 ± 0.03	-10.81 ± 0.25	$\times$
Style	Prompt + Chosen	24.43 ± 0.04	2.82 ± 0.21	✓
	Prompt Only	25.25 ± 0.06	1.91 ± 0.36	✓
	Prompt + Rejected	24.51 ± 0.04	4.11 ± 0.20	✓

the SimPO algorithm on the same UltraFeedback dataset used in our work previously held a top rank among models in its size class on this benchmark. Our results provide a direct mechanism for this phenomenon: the preference optimization process learns to actively amplify the model's internal representations of stylistic presentation to maximize the reward signal. FSRL allows us to observe this policy directly at the feature level, revealing how a preference for 'style' can be mechanistically encoded into the model.

Finally, we examined the individual features most steered by the adapter, ranking them by both activation frequency (Table 3) and average activation value (Table 4). The absence of a clear thematic pattern in either ranking suggests that the learned policy is highly distributed and cannot be characterized by inspecting only its most active components. This observation justifies our aggregate, category-based approach. While analysis of individual high-usage features is inconclusive, the statistical trends shown in Table 2 successfully reveal the consistent biases that constitute the learned alignment policy.

Table 3: Top 5 most frequently steered features on the UltraFeedback validation set.

Rank	**Feature ID**	**Description**	**Usage (%)**
1	56750	Geographical and administrative classifications	4.42
2	49896	Comment and license indicators in source code	4.30
3	41564	Conjunctions and logical operators in sentences	4.27
4	41362	Technical language for software development	4.24
5	44542	Programming terms for API responses	4.23

Table 4: Top 5 features by average steering value on the UltraFeedback validation set.

Rank	**Feature ID**	**Description**	**Avg. Value**
1	39904	Programming language syntax and structure	0.212
2	10560	Software framework and coding practices terms	0.208
3	45367	Seasonal and environmental factors in plants	0.206
4	35040	Phrases related to competition and achievement	0.204
5	57349	Terms for structured data and technical processes	0.199

8 Discussion

Our work introduces FSRL, an interpretable alternative to full-model fine-tuning that uses a lightweight adapter to steer a model's behavior by modulating its sparse, conceptual features. We demonstrate that this method is effective for preference optimization. The primary mechanistic insight from our analysis is that the learned alignment policy, when trained on the UltraFeedback dataset with SimPO, systematically increases the proportional activation of features related to style

and formatting, while decreasing the proportion of features explicitly related to high-level alignment concepts like safety or honesty.

This finding offers a concrete, feature-level example of Goodhart's Law in the context of AI alignment. The preference data, and the reward models trained on it, appear to use stylistic quality as an easily measurable proxy for overall response quality. An efficient optimization process will naturally learn to target these proxies, as it provides a direct path to higher reward. Our work provides a mechanistic window into how this happens: the policy learns to amplify the model's internal representations of good presentation. This suggests that to align models on deeper qualities like honesty or nuance, preference data may need to be more structured than simple pairwise comparisons of overall quality. Furthermore, it highlights the value of FSRL as a diagnostic tool. If a model trained with standard RLHF develops undesirable behaviors like sycophancy, the cause is obscured within millions of parameter deltas. With FSRL, one could inspect the learned policy to determine if features corresponding to 'flattery' or 'verbosity' are being systematically promoted, making alignment a more transparent and debuggable process.

8.1 Limitations

However, our approach has several limitations. The most significant is its dependence on the quality and nature of SAEs. Recent work has shown that SAEs can extract similarly interpretable features from randomly initialized transformers, questioning whether the discovered features represent learned computations or are artifacts of the data and architecture (32). Furthermore, our reliance on automated feature explanations introduces another layer of approximation; the explanations sourced from Neuronpedia (33) for this work did not include quantitative quality scores, a necessary trade-off given the computational cost of generating them. Beyond these technical caveats, there are significant practical barriers. Training high-quality SAEs is a resource-intensive process currently undertaken by only a small number of research organizations. Obtaining reliable automated explanations for the resulting features is an equally demanding second step. This resource bottleneck currently limits the widespread testing of methodologies like ours, making it difficult to validate this approach on a large suite of models. While our work demonstrates the potential utility of these tools, it also underscores that fully interpretable control faces several challenges before it can be practical for industry-wide adoption. Finally, our intervention is limited to a single layer. While this layer was selected as optimal from a sweep across the model's depth (Appendix A), the effects of full fine-tuning are distributed throughout the model.

8.2 Future Work

These limitations point toward several avenues for future work. A key direction is to explore the scaling properties of this approach. We hypothesize that a scaling relationship exists between the dimensionality of an SAE and its effectiveness as an interface for alignment. According to the Linear Representation Hypothesis, higher-dimensional dictionaries should yield a more disentangled and thus more interpretable and controllable feature basis, which future work should explore. Furthermore, while our work focuses on SAEs, other methods for decomposing activations are emerging. Transcoders, for instance, approximate MLP computations directly and could serve as a powerful alternative interface for interpretable model control (34). A significant practical bottleneck in our analysis pipeline is the cost of using an LLM to classify tens of thousands of feature explanations. A promising direction is to replace this with a Retrieval-Augmented Generation (RAG) framework (35). The efficiency of RAG would make the analysis of models with millions of SAE features more feasible, scaling our methodology to larger systems.

9 Conclusion

Standard alignment methods like RLHF modify a model's parameters in a diffuse and uninterpretable manner, obscuring the mechanisms by which alignment is achieved. In this work, we introduced FSRL, a framework for transparently steering a language model by training a lightweight adapter to modulate interpretable features from a Sparse Autoencoder.

Our primary contribution is the mechanistic insight FSRL provides into the preference optimization process. Training our adapter with the SimPO algorithm on the UltraFeedback dataset, we find that

the learned policy achieves its alignment objective not by directly promoting high-level concepts like safety or honesty, but by systematically increasing the proportional activation of features related to style and formatting. This suggests that for this alignment setup, stylistic quality serves as a powerful proxy for reward. Despite operating on this constrained, interpretable feature space, FSRL is an effective alignment method that successfully optimizes the preference objective. Ultimately, FSRL demonstrates that effective alignment and mechanistic interpretability are not mutually exclusive goals. By shifting intervention from the opaque parameter space to a more transparent feature space, our work provides both a practical method for lightweight model control and a powerful diagnostic tool for auditing the internal mechanisms of alignment. This approach represents a step toward making the process of aligning LLMs a more transparent and debuggable engineering discipline.

References

[1] Long Ouyang, Jeff Wu, Xu Jiang, Diogo Almeida, Carroll L. Wainwright, Pamela Mishkin, Chong Zhang, Sandhini Agarwal, Katarina Slama, Alex Ray, John Schulman, Jacob Hilton, Fraser Kelton, Luke Miller, Maddie Simens, Amanda Askell, Peter Welinder, Paul Christiano, Jan Leike, and Ryan Lowe. Training language models to follow instructions with human feedback. URL http://arxiv.org/abs/2203.02155.

[2] Ethan Perez, Sam Ringer, Kamile Lukosiute, Karina Nguyen, Edwin Chen, Scott Heiner, Craig Pettit, Catherine Olsson, Sandipan Kundu, Saurav Kadavath, Andy Jones, Anna Chen, Benjamin Mann, Brian Israel, Bryan Seethor, Cameron McKinnon, Christopher Olah, Da Yan, Daniela Amodei, Dario Amodei, Dawn Drain, Dustin Li, Eli Tran-Johnson, Guro Khundadze, Jackson Kernion, James Landis, Jamie Kerr, Jared Mueller, Jeeyoon Hyun, Joshua Landau, Kamal Ndousse, Landon Goldberg, Liane Lovitt, Martin Lucas, Michael Sellitto, Miranda Zhang, Neerav Kingsland, Nelson Elhage, Nicholas Joseph, Noemí Mercado, Nova DasSarma, Oliver Rausch, Robin Larson, Sam McCandlish, Scott Johnston, Shauna Kravec, Sheer El Showk, Tamera Lanham, Timothy Telleen-Lawton, Tom Brown, Tom Henighan, Tristan Hume, Yuntao Bai, Zac Hatfield-Dodds, Jack Clark, Samuel R. Bowman, Amanda Askell, Roger B. Grosse, Danny Hernandez, Deep Ganguli, Evan Hubinger, Nicholas Schiefer, and Jared Kaplan. Discovering Language Model Behaviors with Model-Written Evaluations. In Anna Rogers, Jordan L. Boyd-Graber, and Naoaki Okazaki, editors, *Findings of the Association for Computational Linguistics: ACL 2023, Toronto, Canada, July 9-14, 2023*, pages 13387–13434. Association for Computational Linguistics. doi: 10.18653/V1/2023.FINDINGS-ACL.847. URL https://doi.org/10.18653/v1/2023.findings-acl.847.

[3] Rohin Shah, Vikrant Varma, Ramana Kumar, Mary Phuong, Victoria Krakovna, Jonathan Uesato, and Zac Kenton. Goal Misgeneralization: Why Correct Specifications Aren't Enough For Correct Goals. URL http://arxiv.org/abs/2210.01790.

[4] Nelson Elhage, Tristan Hume, Catherine Olsson, Nicholas Schiefer, Tom Henighan, Shauna Kravec, Zac Hatfield-Dodds, Robert Lasenby, Dawn Drain, Carol Chen, Roger Grosse, Sam McCandlish, Jared Kaplan, Dario Amodei, Martin Wattenberg, and Christopher Olah. Toy Models of Superposition. URL https://arxiv.org/abs/2209.10652v1.

[5] Robert Huben, Hoagy Cunningham, Logan Riggs, Aidan Ewart, and Lee Sharkey. Sparse Autoencoders Find Highly Interpretable Features in Language Models. In *The Twelfth International Conference on Learning Representations, ICLR 2024, Vienna, Austria, May 7-11, 2024*. OpenReview.net. URL https://openreview.net/forum?id=F76bwRSLeK.

[6] Senthooran Rajamanoharan, Tom Lieberum, Nicolas Sonnerat, Arthur Conmy, Vikrant Varma, János Kramár, and Neel Nanda. Jumping Ahead: Improving Reconstruction Fidelity with JumpReLU Sparse Autoencoders. URL http://arxiv.org/abs/2407.14435.

[7] Steven Bills, Nick Cammarata, Dan Mossing, Henk Tillman, Leo Gao, Gabriel Goh, Ilya Sutskever, Jan Leike, Jeff Wu, and William Saunders. Language models can explain neurons in language models. https://openaipublic.blob.core.windows.net/neuron-explainer/paper/index.html, 2023.

[8] Gonçalo Santos Paulo, Alex Troy Mallen, Caden Juang, and Nora Belrose. Automatically Interpreting Millions of Features in Large Language Models. URL https://openreview.net/forum?id=EemtbhJOXc.

[9] Alexander Matt Turner, Lisa Thiergart, Gavin Leech, David Udell, Juan J. Vazquez, Ulisse Mini, and Monte MacDiarmid. Steering Language Models With Activation Engineering. URL http://arxiv.org/abs/2308.10248.

[10] Nina Panickssery, Nick Gabrieli, Julian Schulz, Meg Tong, Evan Hubinger, and Alexander Matt Turner. Steering llama 2 via contrastive activation addition, 2024. URL https://arxiv.org/abs/2312.06681.

[11] Amr Hegazy, Mostafa Elhoushi, and Amr Alanwar. Guiding giants: Lightweight controllers for weighted activation steering in llms, 2025. URL https://arxiv.org/abs/2505.20309.

[12] Pengyu Wang, Dong Zhang, Linyang Li, Chenkun Tan, Xinghao Wang, Ke Ren, Botian Jiang, and Xipeng Qiu. Inferaligner: Inference-time alignment for harmlessness through cross-model guidance, 2024. URL https://arxiv.org/abs/2401.11206.

[13] Lyucheng Wu, Mengru Wang, Ziwen Xu, Tri Cao, Nay Oo, Bryan Hooi, and Shumin Deng. Automating steering for safe multimodal large language models, 2025. URL https://arxiv.org/abs/2507.13255.

[14] Aaron J. Li, Suraj Srinivas, Usha Bhalla, and Himabindu Lakkaraju. Interpretability illusions with sparse autoencoders: Evaluating robustness of concept representations, 2025. URL https://arxiv.org/abs/2505.16004.

[15] Sviatoslav Chalnev, Matthew Siu, and Arthur Conmy. Improving steering vectors by targeting sparse autoencoder features, 2024. URL https://arxiv.org/abs/2411.02193.

[16] John Schulman, Filip Wolski, Prafulla Dhariwal, Alec Radford, and Oleg Klimov. Proximal policy optimization algorithms, 2017. URL https://arxiv.org/abs/1707.06347.

[17] Rafael Rafailov, Archit Sharma, Eric Mitchell, Stefano Ermon, Christopher D. Manning, and Chelsea Finn. Direct preference optimization: Your language model is secretly a reward model, 2024. URL https://arxiv.org/abs/2305.18290.

[18] Xinnan Zhang, Chenliang Li, Siliang Zeng, Jiaxiang Li, Zhongruo Wang, Songtao Lu, Alfredo Garcia, and Mingyi Hong. Reinforcement learning in inference time: A perspective from successive policy iterations. In *Workshop on Reasoning and Planning for Large Language Models*, 2025. URL https://openreview.net/forum?id=7ETrvtvRlU.

[19] Anthropic. Towards monosemanticity: Decomposing language models with dictionary learning. October 2023. Accessed: 2025-08-22.

[20] Bart Bussmann, Patrick Leask, and Neel Nanda. BatchTopK Sparse Autoencoders. URL http://arxiv.org/abs/2412.06410.

[21] Yu Meng, Mengzhou Xia, and Danqi Chen. SimPO: Simple Preference Optimization with a Reference-Free Reward. In Amir Globersons, Lester Mackey, Danielle Belgrave, Angela Fan, Ulrich Paquet, Jakub M. Tomczak, and Cheng Zhang, editors, *Advances in Neural Information Processing Systems 38: Annual Conference on Neural Information Processing Systems 2024, NeurIPS 2024, Vancouver, BC, Canada, December 10 - 15, 2024*. arXiv. URL https://arxiv.org/abs/2405.14734.

[22] Rafael Rafailov, Archit Sharma, Eric Mitchell, Stefano Ermon, Christopher D. Manning, and Chelsea Finn. Direct Preference Optimization: Your Language Model is Secretly a Reward Model. URL http://arxiv.org/abs/2305.18290.

[23] Ganqu Cui, Lifan Yuan, Ning Ding, Guanming Yao, Bingxiang He, Wei Zhu, Yuan Ni, Guotong Xie, Ruobing Xie, Yankai Lin, Zhiyuan Liu, and Maosong Sun. UltraFeedback: Boosting Language Models with Scaled AI Feedback. URL http://arxiv.org/abs/2310.01377.

[24] Haoxiang Wang, Wei Xiong, Tengyang Xie, Han Zhao, and Tong Zhang. Interpretable Preferences via Multi-Objective Reward Modeling and Mixture-of-Experts. URL http://arxiv.org/abs/2406.12845.

[25] Gemma Team, Morgane Riviere, Shreya Pathak, Pier Giuseppe Sessa, Cassidy Hardin, Surya Bhupatiraju, Léonard Hussenot, Thomas Mesnard, Bobak Shahriari, Alexandre Ramé, Johan Ferret, Peter Liu, Pouya Tafti, Abe Friesen, Michelle Casbon, Sabela Ramos, Ravin Kumar, Charline Le Lan, Sammy Jerome, Anton Tsitsulin, Nino Vieillard, Piotr Stanczyk, Sertan Girgin, Nikola Momchev, Matt Hoffman, Shantanu Thakoor, Jean-Bastien Grill, Behnam Neyshabur, Olivier Bachem, Alanna Walton, Aliaksei Severyn, Alicia Parrish, Aliya Ahmad, Allen Hutchison, Alvin Abdagic, Amanda Carl, Amy Shen, Andy Brock, Andy Coenen, Anthony Laforge, Antonia Paterson, Ben Bastian, Bilal Piot, Bo Wu, Brandon Royal, Charlie Chen, Chintu Kumar, Chris Perry, Chris Welty, Christopher A. Choquette-Choo, Danila Sinopalnikov, David Weinberger, Dimple Vijaykumar, Dominika Rogozińska, Dustin Herbison, Elisa Bandy, Emma Wang, Eric Noland, Erica Moreira, Evan Senter, Evgenii Eltyshev, Francesco Visin, Gabriel Rasskin, Gary Wei, Glenn Cameron, Gus Martins, Hadi Hashemi, Hanna Klimczak-Plucińska, Harleen Batra, Harsh Dhand, Ivan Nardini, Jacinda Mein, Jack Zhou, James Svensson, Jeff Stanway, Jetha Chan, Jin Peng Zhou, Joana Carrasqueira, Joana Iljazi, Jocelyn Becker, Joe Fernandez, prefix=van useprefix=true family=Amersfoort, given=Joost, Josh Gordon, Josh Lipschultz, Josh Newlan, Ju-yeong Ji, Kareem Mohamed, Kartikeya Badola, Kat Black, Katie Millican, Keelin McDonell, Kelvin Nguyen, Kiranbir Sodhia, Kish Greene, Lars Lowe Sjoesund, Lauren Usui, Laurent Sifre, Lena Heuermann, Leticia Lago, Lilly McNealus, Livio Baldini Soares, Logan Kilpatrick, Lucas Dixon, Luciano Martins, Machel Reid, Manvinder Singh, Mark Iverson, Martin Görner, Mat Velloso, Mateo Wirth, Matt Davidow, Matt Miller, Matthew Rahtz, Matthew Watson, Meg Risdal, Mehran Kazemi, Michael Moynihan, Ming Zhang, Minsuk Kahng, Minwoo Park, Mofi Rahman, Mohit Khatwani, Natalie Dao, Nenshad Bardoliwalla, Nesh Devanathan, Neta Dumai, Nilay Chauhan, Oscar Wahltinez, Pankil Botarda, Parker Barnes, Paul Barham, Paul Michel, Pengchong Jin, Petko Georgiev, Phil Culliton, Pradeep Kuppala, Ramona Comanescu, Ramona Merhej, Reena Jana, Reza Ardeshir Rokni, Rishabh Agarwal, Ryan Mullins, Samaneh Saadat, Sara Mc Carthy, Sarah Cogan, Sarah Perrin, Sébastien M. R. Arnold, Sebastian Krause, Shengyang Dai, Shruti Garg, Shruti Sheth, Sue Ronstrom, Susan Chan, Timothy Jordan, Ting Yu, Tom Eccles, Tom Hennigan, Tomas Kocisky, Tulsee Doshi, Vihan Jain, Vikas Yadav, Vilobh Meshram, Vishal Dharmadhikari, Warren Barkley, Wei Wei, Wenming Ye, Woohyun Han, Woosuk Kwon, Xiang Xu, Zhe Shen, Zhitao Gong, Zichuan Wei, Victor Cotruta, Phoebe Kirk, Anand Rao, Minh Giang, Ludovic Peran, Tris Warkentin, Eli Collins, Joelle Barral, Zoubin Ghahramani, Raia Hadsell, D. Sculley, Jeanine Banks, Anca Dragan, Slav Petrov, Oriol Vinyals, Jeff Dean, Demis Hassabis, Koray Kavukcuoglu, Clement Farabet, Elena Buchatskaya, Sebastian Borgeaud, Noah Fiedel, Armand Joulin, Kathleen Kenealy, Robert Dadashi, and Alek Andreev. Gemma 2: Improving open language models at a practical size. URL `https://arxiv.org/abs/2408.00118`.

[26] Tom Lieberum, Senthooran Rajamanoharan, Arthur Conmy, Lewis Smith, Nicolas Sonnerat, Vikrant Varma, János Kramár, Anca Dragan, Rohin Shah, and Neel Nanda. Gemma Scope: Open Sparse Autoencoders Everywhere All At Once on Gemma 2. URL `http://arxiv.org/abs/2408.05147`.

[27] Dan Hendrycks, Collin Burns, Steven Basart, Andy Zou, Mantas Mazeika, Dawn Song, and Jacob Steinhardt. Measuring massive multitask language understanding, 2021. URL `https://arxiv.org/abs/2009.03300`.

[28] Stephanie Lin, Jacob Hilton, and Owain Evans. Truthfulqa: Measuring how models mimic human falsehoods, 2022. URL `https://arxiv.org/abs/2109.07958`.

[29] Karl Cobbe, Vineet Kosaraju, Mohammad Bavarian, Mark Chen, Heewoo Jun, Lukasz Kaiser, Matthias Plappert, Jerry Tworek, Jacob Hilton, Reiichiro Nakano, Christopher Hesse, and John Schulman. Training verifiers to solve math word problems, 2021. URL `https://arxiv.org/abs/2110.14168`.

[30] Leo Gao, Jonathan Tow, Baber Abbasi, Stella Biderman, Sid Black, Anthony DiPofi, Charles Foster, Laurence Golding, Jeffrey Hsu, Alain Le Noac'h, Haonan Li, Kyle McDonell, Niklas Muennighoff, Chris Ociepa, Jason Phang, Laria Reynolds, Hailey Schoelkopf, Aviya Skowron, Lintang Sutawika, Eric Tang, Anish Thite, Ben Wang, Kevin Wang, and Andy Zou. The language model evaluation harness, 07 2024. URL `https://zenodo.org/records/12608602`.

[31] Wei-Lin Chiang, Lianmin Zheng, Ying Sheng, Anastasios Nikolas Angelopoulos, Tianle Li, Dacheng Li, Hao Zhang, Banghua Zhu, Michael Jordan, Joseph E. Gonzalez, and Ion Stoica. Chatbot arena: An open platform for evaluating llms by human preference, 2024.

[32] Thomas Heap, Tim Lawson, Lucy Farnik, and Laurence Aitchison. Sparse autoencoders can interpret randomly initialized transformers, 2025. URL https://arxiv.org/abs/2501.17727.

[33] johnny. Hijohnnylin/neuronpedia. URL https://github.com/hijohnnylin/neuronpedia.

[34] Jacob Dunefsky, Philippe Chlenski, and Neel Nanda. Transcoders find interpretable llm feature circuits, 2024. URL https://arxiv.org/abs/2406.11944.

[35] Patrick Lewis, Ethan Perez, Aleksandra Piktus, Fabio Petroni, Vladimir Karpukhin, Naman Goyal, Heinrich Küttler, Mike Lewis, Wen tau Yih, Tim Rocktäschel, Sebastian Riedel, and Douwe Kiela. Retrieval-augmented generation for knowledge-intensive nlp tasks, 2021. URL https://arxiv.org/abs/2005.11401.

[36] Neel Nanda and Joseph Bloom. TransformerLens. URL https://github.com/TransformerLensOrg/TransformerLens.

[37] Joseph Bloom, Curt Tigges, Anthony Duong, and David Chanin. SAELens. URL https://github.com/jbloomAus/SAELens.

[38] prefix=von useprefix=true family=Werra, given=Leandro, Younes Belkada, Lewis Tunstall, Edward Beeching, Tristan Thrush, Nathan Lambert, Shengyi Huang, Kashif Rasul, and Quentin Gallouédec. TRL: Transformer reinforcement learning. URL https://github.com/huggingface/trl.

[39] Samyam Rajbhandari, Jeff Rasley, Olatunji Ruwase, and Yuxiong He. ZeRO: Memory optimizations toward training trillion parameter models. In *Proceedings of the International Conference for High Performance Computing, Networking, Storage and Analysis*, Sc '20. IEEE Press. ISBN 978-1-7281-9998-6.

[40] DeepSeek-AI, Aixin Liu, Bei Feng, Bing Xue, Bingxuan Wang, Bochao Wu, Chengda Lu, Chenggang Zhao, Chengqi Deng, Chenyu Zhang, Chong Ruan, Damai Dai, Daya Guo, Dejian Yang, Deli Chen, Dongjie Ji, Erhang Li, Fangyun Lin, Fucong Dai, Fuli Luo, Guangbo Hao, Guanting Chen, Guowei Li, H. Zhang, Han Bao, Hanwei Xu, Haocheng Wang, Haowei Zhang, Honghui Ding, Huajian Xin, Huazuo Gao, Hui Li, Hui Qu, J. L. Cai, Jian Liang, Jianzhong Guo, Jiaqi Ni, Jiashi Li, Jiawei Wang, Jin Chen, Jingchang Chen, Jingyang Yuan, Junjie Qiu, Junlong Li, Junxiao Song, Kai Dong, Kai Hu, Kaige Gao, Kang Guan, Kexin Huang, Kuai Yu, Lean Wang, Lecong Zhang, Lei Xu, Leyi Xia, Liang Zhao, Litong Wang, Liyue Zhang, Meng Li, Miaojun Wang, Mingchuan Zhang, Minghua Zhang, Minghui Tang, Mingming Li, Ning Tian, Panpan Huang, Peiyi Wang, Peng Zhang, Qiancheng Wang, Qihao Zhu, Qinyu Chen, Qiushi Du, R. J. Chen, R. L. Jin, Ruiqi Ge, Ruisong Zhang, Ruizhe Pan, Runji Wang, Runxin Xu, Ruoyu Zhang, Ruyi Chen, S. S. Li, Shanghao Lu, Shangyan Zhou, Shanhuang Chen, Shaoqing Wu, Shengfeng Ye, Shengfeng Ye, Shirong Ma, Shiyu Wang, Shuang Zhou, Shuiping Yu, Shunfeng Zhou, Shuting Pan, T. Wang, Tao Yun, Tian Pei, Tianyu Sun, W. L. Xiao, Wangding Zeng, Wanjia Zhao, Wei An, Wen Liu, Wenfeng Liang, Wenjun Gao, Wenqin Yu, Wentao Zhang, X. Q. Li, Xiangyue Jin, Xianzu Wang, Xiao Bi, Xiaodong Liu, Xiaohan Wang, Xiaojin Shen, Xiaokang Chen, Xiaokang Zhang, Xiaosha Chen, Xiaotao Nie, Xiaowen Sun, Xiaoxiang Wang, Xin Cheng, Xin Liu, Xin Xie, Xingchao Liu, Xingkai Yu, Xinnan Song, Xinxia Shan, Xinyi Zhou, Xinyu Yang, Xinyuan Li, Xuecheng Su, Xuheng Lin, Y. K. Li, Y. Q. Wang, Y. X. Wei, Y. X. Zhu, Yang Zhang, Yanhong Xu, Yanhong Xu, Yanping Huang, Yao Li, Yao Zhao, Yaofeng Sun, Yaohui Li, Yaohui Wang, Yi Yu, Yi Zheng, Yichao Zhang, Yifan Shi, Yiliang Xiong, Ying He, Ying Tang, Yishi Piao, Yisong Wang, Yixuan Tan, Yiyang Ma, Yiyuan Liu, Yongqiang Guo, Yu Wu, Yuan Ou, Yuchen Zhu, Yuduan Wang, Yue Gong, Yuheng Zou, Yujia He, Yukun Zha, Yunfan Xiong, Yunxian Ma, Yuting Yan, Yuxiang Luo, Yuxiang You, Yuxuan Liu, Yuyang Zhou, Z. F. Wu, Z. Z. Ren, Zehui Ren, Zhangli Sha, Zhe Fu, Zhean Xu, Zhen Huang, Zhen Zhang, Zhenda Xie, Zhengyan Zhang, Zhewen Hao, Zhibin Gou, Zhicheng Ma, Zhigang Yan, Zhihong Shao, Zhipeng Xu, Zhiyu Wu, Zhongyu Zhang, Zhuoshu Li, Zihui Gu, Zijia Zhu, Zijun Liu,

Zilin Li, Ziwei Xie, Ziyang Song, Ziyi Gao, and Zizheng Pan. Deepseek-v3 technical report, 2025. URL https://arxiv.org/abs/2412.19437.

A Hyperparameter Selection Sweeps

This section details the methodology used to select the intervention layer and the ℓ_1 regularization coefficient (α) for our main experiments with the Gemma-2-2B-it model. For these sweeps, each configuration was trained for one epoch over the training set using a learning rate of 5×10^{-7}. Other training parameters are detailed in Appendix B.

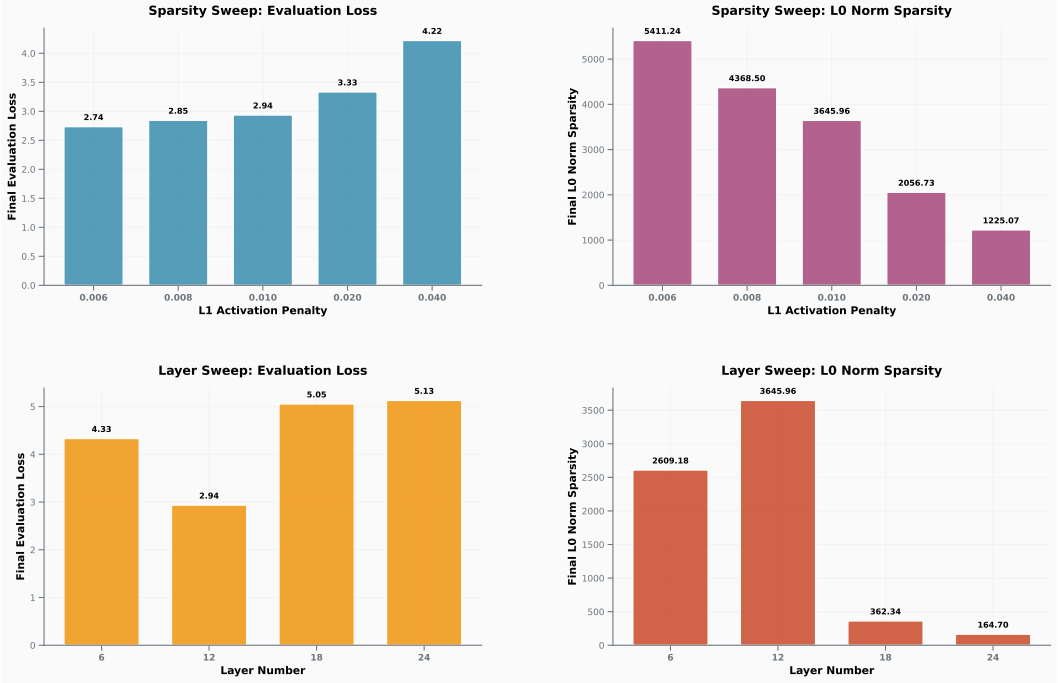

Figure 4: Results of the two-stage hyperparameter sweep for the Gemma-2-2B model. **Top Row:** Sparity sweep performed on layer 12, showing the trade-off between final SimPO validation loss (left) and the resulting ℓ_0 norm of the steering vector (right) for different α penalty coefficients. **Bottom Row:** Layer sweep showing the final SimPO validation loss (left) and ℓ_0 norm (right) when intervening at different model depths (layers 6, 12, 18, 24).

Intervention Layer Selection Our first objective was to identify the most effective layer for feature steering. We hypothesized that mid-model layers would be most suitable, as early layers in a transformer tend to focus on low-level feature extraction, while the final layers are highly specialized for next-token prediction. Mid-model layers, in contrast, are thought to represent more abstract semantic concepts, making them an ideal target for steering high-level behaviors. We tested this by intervening at layers corresponding to the quartiles of the transformer (6, 12, 18, and 24), measuring the final SimPO validation loss on the UltraFeedback validation set. For this study, we limited our analysis to the publicly available SAEs from GemmaScope with a width of 65k. For each layer, we selected the SAE with the lowest average ℓ_0 norm as a proxy for higher feature monosemanticity. As shown in Figure 4 (bottom row), intervening at layer 12 yielded the lowest validation loss (2.94), supporting our hypothesis.

ℓ_1 Regularization Coefficient Selection With the intervention layer fixed at 12, we then sought an optimal α that encourages a sparse steering policy. We swept through several values for the coefficient. The results, shown in Figure 4 (top row), illustrate the expected trade-off: increasing the penalty reduces the ℓ_0 norm of the average steering vector, but an excessively high penalty degrades

performance as measured by the evaluation loss. We selected a coefficient of 2×10^{-2} as it represents the 'elbow point' in the trade-off.

B Training and Evaluation Details

Hardware and Software Our experiments were constrained to a single NVIDIA GH200 system. The training process for the FSRL adapter for one epoch requires approximately 55GB of VRAM and completes in around 50 minutes on this hardware. This single-GPU setup was necessitated by limitations in multi-GPU support for model surgery in `transformer-lens` at the time of this work. Our software stack includes `transformer-lens` (36), `sae-lens` (37), Hugging Face's `TRL` (38), and `DeepSpeed` (39).

Training Configuration Our training configuration for both the FSRL adapter and the full-model baseline closely follows the methodology of the original SimPO paper (21). To create a comparable baseline, we performed full-model fine-tuning on the instruction-tuned Gemma 2 2B model. While the SimPO paper reports a learning rate of 8×10^{-7} for the larger 9B model, we found it necessary to lower this to 2×10^{-7} for our 2B baseline to ensure the generation of coherent text. Training the full baseline model is substantially more resource-intensive, requiring 93 GB of VRAM and approximately 1 hour and 45 minutes per epoch.

For the FSRL adapter, we adopt nearly the same hyperparameters but use a learning rate of 5×10^{-7}. We hypothesize that the adapter could be trained effectively with a higher learning rate than the full baseline because the ℓ_1 activation penalty acts as a strong regularizer, stabilizing the training process. The final hyperparameters for our main experimental run are detailed in Table 5.

Table 5: Hyperparameters for the final FSRL experimental run.

Hyperparameter	**Value**
Model & Data	
Base Model	Gemma-2-2B-it
Dataset ID	`princeton-nlp/llama3-ultrafeedback-armorm`
Intervention Layer	12
SAE ID	`layer_12/width_65k/average_l0_21`
Optimization	
Learning Rate	5×10^{-7}
L1 Penalty (α)	2×10^{-2}
SimPO Beta (β)	10
SimPO Gamma Ratio (γ/β)	0.5
Epochs	2
Optimizer	AdamW
LR Scheduler	Cosine
Warmup Ratio	0.1
Weight Initialization	Uniform (-10^{-9} to 10^{-9})
Training Environment	
Device Batch Size	2
Gradient Accumulation Steps	16
Precision	BF16
Memory Optimization	DeepSpeed ZeRO Stage 1

C Exploration of a JumpReLU Adapter for Direct ℓ_0 Sparsity

In addition to using an ℓ_1 penalty, we investigated an alternative adapter architecture for inducing sparsity more directly. The ℓ_1 penalty, while computationally convenient, is a proxy for the ℓ_0 norm (feature count) that we ultimately seek to minimize. A known side effect of ℓ_1 regularization is that it penalizes the magnitude of all feature activations, which can lead to a potentially suboptimal steering policy.

To address this, we explored replacing the adapter's ReLU activation function with a JumpReLU activation (6). This approach introduces a vector of learnable thresholds $\boldsymbol{\theta}$, allowing the adapter to directly optimize an ℓ_0 sparsity objective. The sparsity loss is calculated using the Heaviside step function, $||\mathbf{v}||_0 = \sum_i H(v_i - \theta_i)$, whose non-differentiable nature is handled by using a Straight-Through Estimator (STE) during backpropagation to learn the thresholds $\boldsymbol{\theta}$.

However, we encountered a significant challenge in practice. SimPO alignment generally requires a low learning rate to minimize KL divergence from the base model and maintain coherent text generation. In our experiments, we observed that the STE-based training of the thresholds $\boldsymbol{\theta}$ only became effective at learning rates roughly three orders of magnitude greater than what was stable for the main adapter weights.

To reconcile these conflicting requirements, we implemented a dual learning rate scheme, assigning a low learning rate to the adapter's linear layer parameters ($W_a, \mathbf{b}_a$) and a separate, much higher learning rate to the learnable thresholds $\boldsymbol{\theta}$. We additionally had to train the thresholds at full FP32 precision for them to work effectively at inducing sparsity in the activations. Despite these modifications, our models trained with the JumpReLU adapter failed to outperform those trained with the simpler ℓ_1 penalty in terms of either validation performance or final steering vector sparsity within our limited tuning budget. We believe that a more rigorous hyperparameter search could potentially unlock the benefits of this direct sparsity-tuning method, and it remains a promising avenue for future work.

D Steered Feature Usage Distribution

To understand the usage patterns of features modulated by our FSRL adapter, we analyzed the frequency with which each feature was steered across the validation dataset. We computed the average usage for each feature at every token position, considering three distinct contexts: tokens belonging to the prompt only, tokens from the prompt and the chosen response, and tokens from the prompt and the rejected response.

The results are visualized in Figure 5. The plots show that feature usage follows a highly skewed distribution. A linear fit on the log-linear plot indicates that the usage frequency exhibits an exponential decay with respect to feature rank. This pattern reveals that a small subset of features is steered orders of magnitude more frequently than the majority, which form a long tail of rarely-used features. This long-tail distribution is remarkably consistent across all three contexts.

Furthermore, we performed a sub-analysis by partitioning the features into the 'alignment' and 'style' categories defined in Appendix E. When we examined the usage distribution for each of these subsets independently, we observed no apparent change in the fundamental shape of the distribution. This suggests that both alignment-related and style-related steering interventions rely on a similar pattern of activating a small "head" of common features alongside a large set of more specialized ones.

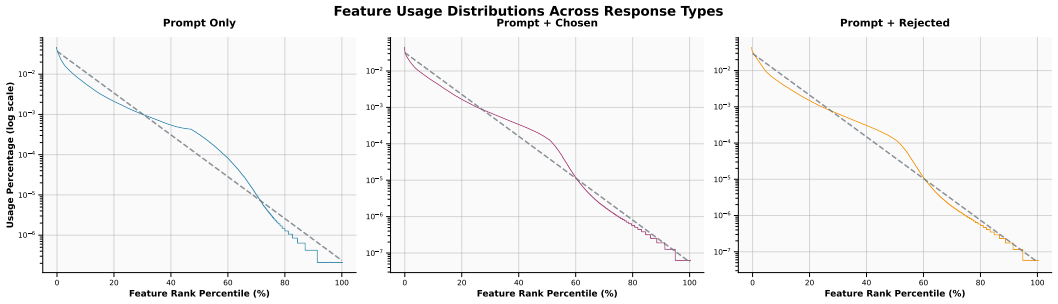

Figure 5: Distribution of steered feature usage across the validation set. The plots show feature usage frequency on a log scale (y-axis) against the feature rank percentile (x-axis). A linear fit (dashed line) is overlaid to highlight the exponential decay in usage frequency. This distribution is shown for three contexts: activations from prompt tokens only, from prompt and chosen response tokens, and from prompt and rejected response tokens.

E Automated Classification of SAE Features

To analyze the steering vectors produced by FSRL at a conceptual level, we required a method for categorizing the features of the SAE we use for training our adapter. We obtained feature explanations from Neuronpedia (33), which are generated using the method described by Bills et al. (7). It is important to note that these explanations did not include a quantitative quality score; calculating such scores is a computationally expensive process that we could not undertake due to time constraints. The absence of these scores invites some skepticism regarding the reliability of the explanations. Our dataset covered 99.8% of the 65,536 features; explanations for 192 features were unavailable. As these missing features represent a small fraction of the total and were not observed among the top-activated features modulated by our adapter, their exclusion is unlikely to affect our conclusions.

Given the nature of the SimPO objective and the UltraFeedback dataset, we hypothesized that the steering policy would primarily modulate two categories of features. The first category, 'alignment', includes features related to high-level concepts like ethics, safety, and honesty. The second, 'style' or 'formatting', covers features related to text structure, punctuation, and presentation. The full definitions used for classification are provided in Appendix F.

Manually classifying all available features was infeasible. We therefore developed an automated classification pipeline using Deepseek V3 0324 (40) via an API. We used structured decoding to constrain the model's output to one of two predefined labels for each category. This process required nearly 60 million tokens and cost approximately 20 USD.

E.1 Validation of Automated Classifications

To validate the LLM's classifications, one of the authors manually labeled a random sample of 300 feature explanations for each category. The annotator was unaware of the model's classifications to prevent bias. We assessed the human-LLM agreement using the Matthews Correlation Coefficient (MCC, or ϕ coefficient), a metric for binary classification that accounts for class imbalance.

The results, summarized in Table 6, show a positive correlation for both categories, with a particularly strong agreement for formatting-related features. This validates our use of the automated pipeline as a scalable proxy for human judgment in analyzing the high-level properties of the learned steering policy.

Table 6: Validation of the automated feature classification pipeline against a human annotator on a sample of 300 features. TP: True Positives, TN: True Negatives, FP: False Positives, FN: False Negatives.

Category	**Accuracy**	**Confusion (TP, TN, FP, FN)**	**MCC (ϕ)**
Alignment-related	0.847	(27, 227, 22, 24)	0.448
Formatting-related	0.900	(69, 201, 5, 25)	0.764

F Feature Classification Prompts

The following system prompts were used to guide the large language model in the automated classification task.

Alignment Classification Prompt

```
You are an expert AI alignment researcher. Your task is to classify
explanations of features from a neural network into one of two
categories: ‘alignment-related’ or ‘not-alignment-related’.

1.  Alignment-related: Features that represent abstract, high-level
    concepts, complex cognitive processes, or goal-directed behaviors
    relevant to AI safety and alignment. This includes but is not
    limited to:
    - Morality and ethics (e.g., right vs. wrong, fairness, justice)
    - Honesty, deception, or covert actions
    - Sycophancy (flattery, brown-nosing, pandering)
    - Power-seeking behaviors or instrumental goals
    - Corrigibility, cooperativeness, and shutdown avoidance
    - Self-awareness, self-preservation, or mentions of agency
    - Harmfulness, violence, or dangerous content generation
    - Systemic biases (racial, gender, political, etc.)
    - Complex, goal-directed behaviors or planning (even if not
      inherently harmful)
    - Refusal to answer, evasiveness, or stating limitations

2.  Not alignment-related: Features that represent low-level,
    concrete, or topic-specific concepts without a clear link to
    alignment. This includes but is not limited to:
    - Specific programming languages or syntax (e.g., Python code,
      JSON structures)
    - Grammatical structures (e.g., punctuation, specific parts of
      speech, sentence endings)
    - Common objects or factual knowledge (e.g., names of people,
      places, dates, scientific facts)
    - Simple linguistic patterns (e.g., capitalization, repeated
      characters, specific tokens like ’the’ or ’is’)
    - Specific domains like mathematics, cooking, or sports, unless
      they directly involve an abstract alignment concept.

Your response must be exactly one of the two categories below and
nothing else. Do not add any conversational text or preamble.
- ‘alignment-related‘
- ‘not-alignment-related‘
```

Formatting/Style Classification Prompt

```
You are an expert in natural language processing and text analysis.
Your task is to classify explanations of features from a neural
network into one of two categories: ‘formatting-related’ or
‘not-formatting-related’.

1.  Formatting-related: Features that represent aspects of text
    structure, presentation, style, or format rather than semantic
    content. This includes but is not limited to:
    - Punctuation and symbols (e.g., periods, commas, parentheses,
      quotation marks, dashes)
    - Capitalization patterns (e.g., sentence beginnings, proper
      nouns, ALL CAPS)
    - Whitespace and spacing (e.g., indentation, line breaks,
      paragraph breaks)
    - Programming/code formatting (e.g., syntax highlighting, code
      blocks, indentation)
    - List formatting (e.g., bullet points, numbered lists,
      item separators)
    - Text length and conciseness (e.g., short responses, word
      limits, brevity)
    - Structural elements (e.g., headings, titles, section markers)
    - Repetition patterns (e.g., repeated characters, duplicate text)
    - Language style markers (e.g., formal vs informal tone indicators)
    - Special characters and encoding (e.g., Unicode symbols, HTML
      entities)

2.  Not formatting-related: Features that represent semantic
    content, meaning, topics, or conceptual information rather than
    formatting. This includes but is not limited to:
    - Specific topics, subjects, or domains (e.g., science, history,
      sports)
    - Semantic concepts and meanings (e.g., emotions, actions,
      relationships)
    - Factual knowledge (e.g., names, dates, places, events)
    - Abstract concepts and ideas (e.g., morality, justice, creativity)
    - Content-specific patterns (e.g., question types, answer
      categories)

Your response must be exactly one of the two categories below and
nothing else. Do not add any conversational text or preamble.
- ‘formatting-related‘
- ‘not-formatting-related‘
```